Buffering of atmospheric nanoparticle growth by temperature-dependent shifts in molecular composition, volatility and diffusivity

Zhiqiang Zhang[1], Hyun Gu Kang[1], Ulrich Pöschl[1], and Thomas Berkemeier[1]

[1]Multiphase Chemistry Department, Max Planck Institute for Chemistry, Hahn-Meitner-Weg 1, 55128 Mainz, Germany

Correspondence: Thomas Berkemeier (t.berkemeier@mpic.de)

Abstract

Aerosols have a profound influence on climate and human health, but new particle formation in the atmosphere has remained a scientific conundrum. In particular, the growth rates of atmospheric nanoparticles are often smaller and less dependent on condensable vapor concentration than expected. Here, we take a new integrative approach to analyze observational data from field measurements and chamber experiments, which were previously unexplained and appeared inconsistent with theory and model predictions. We show that the observed growth rates can be predicted when the temperature dependence and multiphase kinetics of gas-particle partitioning are resolved. Slow surface-to-bulk transport limits the rates of vapor uptake by semi-solid particles with low diffusivity, whereas shifts in the volatility distribution following the Clausius-Clapeyron equation enhance growth rates at low temperature and concentration levels. These antagonistic effects lead to an effective buffering of the organic vapor concentration dependence of nanoparticle growth in secondary organic aerosols. Our study reveals how counteracting temperature dependencies of organic vapor oxidation, volatility and diffusivity can explain the convergence of growth rates around a few nanometers per hour under widely varying atmospheric conditions.

1 Introduction

Atmospheric aerosols consisting of airborne particles in the nanometer to micrometer size range have a strong influence on air quality, public health, and climate (IPCC, 2023; WHO, 2023). Large fractions of airborne fine particulate matter consist of secondary organic aerosols (SOA) formed by gas-to-particle conversion of organic precursor molecules in the atmosphere (Jimenez et al., 2009; Hallquist et al., 2009; Riipinen et al., 2011; Shrivastava et al., 2017). Over the past decades, numerous studies have investigated atmospheric new particle formation and growth (Kulmala et al., 2004, 2014; Stolzenburg et al., 2023). The rates of nanoparticle growth, however, have remained enigmatic and constitute a gap in the scientific understanding and assessment of atmospheric aerosols and their effects on health and climate (Bianchi et al., 2016; Gordon et al., 2017; Kulmala et al., 2022). In particular, the growth rates of atmospheric SOA particles observed in field measurements are fairly uniform around 1-10 nm h^{-1} and exhibit a relatively weak dependence on measured organic vapor concentrations that vary by multiple

orders of magnitude (Stolzenburg et al., 2018; Yli-Juuti et al., 2020; Stolzenburg et al., 2025). Computational models utilizing volatility basis sets (VBS; Donahue et al., 2006, 2011; Bhattacharyya et al., 2025) were found to reproduce observations under a variety of conditions, while under- or over-predicting nanoparticle growth rates measured in other instances (Stolzenburg et al., 2018; Mohr et al., 2019; Qiao et al., 2021; Stolzenburg et al., 2022; Dada et al., 2023; Cai et al., 2026).

Under atmospheric conditions, organic aerosol particles are expected to exist in highly viscous or semi-solid phase states and may even exhibit an amorphous solid (glassy) state depending on chemical composition, temperature, and humidity (Zobrist et al., 2008; Mikhailov et al., 2009; Virtanen et al., 2010; Koop et al., 2011; Renbaum-Wolff et al., 2013; Shiraiwa et al., 2017; Reid et al., 2018). Accordingly, the molecular diffusivity in SOA particles can vary over a wide range from more than 10^{-10} cm^2 s^{-1} (liquid) to less than 10^{-21} cm^2 s^{-1} (glassy), which influences the kinetics of mass transport, gas uptake, and partitioning (Shiraiwa et al., 2011; Berkemeier et al., 2013; Shiraiwa et al., 2014; Zaveri et al., 2018). Earlier studies have shown that diffusivity-limitations can affect the water uptake, heterogeneous chemical transformation, evaporation, and size distribution of organic aerosol particles (Pfrang et al., 2011; Zhou et al., 2013; Arangio et al., 2015; Berkemeier et al., 2014, 2016; Mu et al., 2018; Zaveri et al., 2020; Berkemeier et al., 2020; Schervish et al., 2026; Kang et al., 2026).

Here, we re-analyze observational data of nanoparticle growth from field measurements in the boreal forest (Hyytiälä, Finland) and from sophisticated laboratory experiments (CERN CLOUD), utilizing a new kinetic multilayer model of multiphase chemistry (KM3C) that resolves the reactivity, diffusivity, and concentration gradients of different chemical species across the gas phase, condensed phase, and the interface between them. We demonstrate that SOA nanoparticle growth can be accurately predicted when the relevant thermodynamic and kinetic aspects of aerosol properties, processes, and temperature dependencies are taken into account in an integrative approach of data analysis and numerical modeling.

2 Results and Discussion

Figure 1 illustrates how the elucidation of condensed-phase diffusivity and concentration profiles inside SOA particles resolves previously unexplained discrepancies between field measurements and model predictions of condensable organic vapor concentrations and nanoparticle growth rates. As shown in Fig. 1a and reported by Stolzenburg et al. (2025), nanoparticle growth rates observed in the boreal forest summer (blue markers) were substantially lower than those predicted with a two-film model (Zaveri et al., 2014) assuming quasi-liquid particles with high diffusivity (>10^{-15} cm^2 s^{-1}, solid brown line and shading). In their modeling approach, Stolzenburg et al. (2025) considered uncertainties and variations related to condensable vapor concentration measurements, activity coefficients, decomposition reactions, and reduced diffusivity (10^{-18} cm^2 s^{-1}, dashed brown line), but they did not reach agreement with the measurement results and highlighted incomplete mass closure.

In contrast, our kinetic multilayer model KM3C is able to reproduce the observed growth rates assuming a diffusivity characteristic for highly viscous, nearly glassy semi-solid substances (10^{-20} cm^2 s^{-1}) and otherwise identical model parameters such as the time-dependent concentrations of condensable organic vapors, their enthalpies of vaporization, and the treatment of the Kelvin effect (Supplementary Information, Sect. S1). Using the same diffusivity in the two-film model published by Stolzenburg et al. (2025), we obtain closure for larger particles sizes, but not below 3 nm (brown dotted line), which indicates

that details of interfacial mass transport, molecular diffusion, and differential concentration gradients as resolved in KM3C are relevant for the kinetics of atmospheric nanoparticle growth.

Figure 1c illustrates how low diffusivity leads to the development of differential concentration gradients inside the nanoparticle as described in KM3C, where the outer layers contain higher fractions of relatively more volatile compounds (low-volatile organic compounds, LVOC) compared to the inner layers, which in turn show higher fractions of relatively less volatile compounds (ultra low-volatile organic compounds, ULVOC). This is consistent with the role of ULVOC in new particle formation and nucleation, respectively (Dada et al., 2023; Donahue et al., 2026). The low diffusivity leads to an enrichment of relatively more volatile compounds at the surface, decelerates their uptake into the particle bulk (surface-to-bulk transport), and delays the equilibration of gas-particle partitioning. These effects keep the particle growth rate lower than expected under the assumption of a well-mixed and thus rapidly equilibrating particle phase (Fig. S1). An analysis of the temporal evolution of particle growth, composition and concentration gradients shows that the particle core largely retains the initial composition dominated by relatively less volatile vapors (ELVOC, ULVOC) when diffusivity is low (Fig. S2, panels a-c). In a sensitivity test with high diffusivity and otherwise unchanged conditions, relatively more volatile vapors (SVOC, LVOC) are readily taken up and well-mixed throughout the particle (Fig. S2, panels d-f).

As illustrated in Fig. 1b, nanoparticle growth observed in the boreal forest spring was well captured by both the two-film model of Stolzenburg et al. (2025) as well as our multilayer model with higher diffusivity (10^{-15} cm^2 s^{-1}, solid blue line and shading). Under these conditions, the multilayer model shows a well-mixed particle bulk without differential concentration gradients (Fig. 1d), indicating that the growth rates observed and simulated under these conditions are not limited by molecular diffusivity. We find that the sensitivity to particle phase state and diffusivity is less pronounced in the springtime scenario (Fig. S3), and KM3C captures the spring data within experimental errors also at a diffusivity of 10^{-18} cm^2 s^{-1} (dashed blue line).

The diffusion properties of complex SOA mixtures have not yet been constrained with high precision, but the occurrence of different phase states and diffusivities of SOA nanoparticles in the investigated growth events is consistent with earlier studies. These studies showed that SOA particles formed in boreal, mid-latitude, and tropical forests vary between liquid, semi-solid and glassy phase states depending on aerosol composition, particle size, and ambient conditions such as temperature and humidity (Mikhailov et al., 2009; Virtanen et al., 2010; Koop et al., 2011; Saukko et al., 2012; Renbaum-Wolff et al., 2013; Cheng et al., 2015; Bateman et al., 2016; Slade et al., 2019; Artaxo et al., 2022). While the relative humidity during the two particle growth events displayed in Fig. 1 was essentially the same ($\sim$ 50% RH), the ambient temperature was higher in August (17.5°C) than in April (3.8°C, Stolzenburg et al., 2025). At elevated temperatures, organic compounds need higher molecular masses and oxygen contents to reach low-enough vapor pressures for condensing and partitioning largely into the particle phase (Donahue et al., 2011; Shiraiwa et al., 2014; Bilde et al., 2015; Li et al., 2016). Moreover, photochemical aging may proceed faster in summer and has been shown to increase the viscosity of organic aerosols (Antossian et al., 2026; Golay et al., 2026). Due to differences in chemical composition and because the enthalpies of vaporization can exceed activation energies of diffusion (Epstein et al., 2010; Kiland et al., 2019), the diffusivity in organic matter condensing at high temperature may be lower than in organic matter condensing at low temperature. The volatilities of organic compounds show Arrhenius-behavior following the Clausius-Clapeyron equation, but the viscosity of organic liquids approaching the glass transition generally

exhibits super-Arrhenius behavior following the Vogel–Fulcher–Tammann equation (Bilde et al., 2015; Shiraiwa et al., 2017). In semi-solids, activation energies of diffusion may be smaller than enthalpies of vaporization, which would entail a hardening of organic aerosols towards higher temperatures. For glassy organics, however, activation energies of diffusion may be larger than enthalpies of vaporization and the dependence may reverse: a liquefaction of organic aerosols towards higher temperatures.

To obtain quantitative estimates of these effects, we employ semi-empirical parameterizations of SOA diffusivity established by Li et al. (2020) and Kang et al. (2026), which relate glass transition temperatures, viscosities and self-diffusion coefficients to the volatilities of organic compounds (Sect. S7). Inserting these parameterizations in KM3C, we can calculate diffusivities for each particle layer as a function of chemical composition and time (Kang et al., 2026). As detailed in Fig. S4, the model simulations following Li et al. (2020) predict glassy solid nanoparticle phase states with glass transition temperatures (T_g) well above 300 K and diffusivities smaller than 10^{-20} cm^2 s^{-1} throughout the investigated growth events in summer and spring. Plasticizer effects of water and sulfate were taken into account (Sect. S7; Koop et al., 2011; Dette and Koop, 2015), but did not alter the modeling results substantially. The model simulations following Kang et al. (2026) in Fig. S5 predict time-dependent and radially inhomogenous semi-solid phase states with diffusivities that are initially lower in summer than in spring, and of comparable magnitude overall (10^{-20} to 10^{-18} cm^2 s^{-1}). In both scenarios, the diffusivity increases over time as the particles grow by condensation of relatively more volatile compounds (Figs. S4, S5). To explore the potential influence of nanosize effects following Cheng et al. (2015), we combined the parameterization of Li et al. (2020) with data measured by Mahant et al. (2024) and find that glass transition temperatures decrease substantially ($\Delta T_g \sim 40 - 50$ K), but not below 300 K. As the nanoparticle size effect declines towards larger particle sizes (Fig. S6), condensation of higher volatile vapors offsets this change, leading to a near-constant T_g around 320 K. Additional effects such as enhanced mobility in the surface layers of solid particles (quasi-liquid layers) warrant further investigation in follow-up studies (McNeill et al., 2006; Stevenson and Wolynes, 2008; Tian et al., 2022).

Overall, the available data and parameterizations suggest that nanoparticle formation and growth by condensation of low-volatile organic vapors indeed yields nanoparticles with high viscosity and low diffusivity. Despite the remaining uncertainties in predicting these molecular properties, our model results demonstrate that kinetic limitations related to particle-phase diffusivity of condensable organic vapors offer a plausible, coherent, and quantitative explanation for previously unexplained observations.

Figure 2 shows nanoparticle growth rates measured under very well defined conditions in the CERN CLOUD chamber (Stolzenburg et al., 2018). For particles in the diameter range of 1.5 to 3 nm (Fig. 2a), the growth rates observed at 5°C are near the kinetic limit derived by Stolzenburg et al. (2025) from the concentration of oxidized organic molecules (OOMs) measured by nitrate chemical ionization mass spectrometry (NO3-CIMS). The rates observed at -25°C and 25°C, however, are well above and below the kinetic limit (OOMs) line, respectively, and were not captured by this modeling approach (Stolzenburg et al., 2025). In the particle size range of 3 to 7 nm (Fig. 2b), the observed growth rates are close to the reported kinetic limit at 5°C and 25°C, but again much higher at -25°C.

When considering only the OOMs measured by NO3-CIMS (Fig. S7), our kinetic multilayer model was not able to reproduce the observed growth rates. Thus, we included organic vapors measured by proton-transfer reaction time-of-flight mass

spectrometry (PTR3; Stolzenburg et al., 2018) and integrated the Clausius-Clapeyron equation in KM3C to describe the temperature-dependent volatility distribution of organic vapors (Supplementary Information, Sect. S1). This approach captures both the concentration dependence and the temperature dependence of the measured nanoparticle growth rates as illustrated in Figs. 2a,b. In accordance with the VBS modeling approach of Stolzenburg et al. (2022), our kinetic model calculations confirm that comprehensive measurement techniques and data are needed to cover the full range and variability of condensable organic vapors. This includes semi-volatile organic compounds (SVOC) that can substantially contribute to nanoparticle growth at -25°C even if their contribution is negligible at +25°C (Fig. S8). As shown by Riva et al. (2019); Mohr et al. (2019); Dada et al. (2023), full coverage of condensable organic vapors by mass spectrometry requires suitable instrumentation and ionization techniques as the sensitivity towards compounds with different degrees of oxygenation can vary strongly.

As illustrated in Fig. 2, the growth rates observed at high temperature in the CERN CLOUD chamber experiments of α-pinene ozonolysis under dark conditions (25°C, yellow bands and data points) are best reproduced assuming relatively low diffusivity for particles smaller than 3 nm (Fig. 2a) and higher diffusivity for larger nanoparticles (Fig. 2b). In contrast, reproducing the boreal summertime field observations requires low diffusivity for the entire size range up to 11 nm (Fig. 1a). These differences in diffusivity can be plausibly attributed to differences in particle composition and chemical aging. As shown in Fig. S2, smaller particles contain higher proportions of organic compounds with low intrinsic volatility (ELVOC/ULVOC), while the uptake and partitioning of relatively more volatile compounds (SVOC/LVOC) tend to reduce the viscosity and increase the diffusivity of larger particles. Intrinsic volatility is often characterized by the saturation mass concentration at a standard temperature of 298 K (C^*_{298}, Schervish and Donahue, 2020; Donahue et al., 2026).

The molecular composition of SOA particles formed by dark ozonolysis of α-pinene (CERN CLOUD) is likely not the same as for particles formed in summertime boreal forest air (Hyytiälä), which may be influenced by other volatile precursors (monoterpenes, sesquiterpenes; Hellén et al., 2018) and photo-oxidants including OH radicals. Furthermore, sunlight and atmospheric photochemistry may promote condensed-phase reactions that can enhance the formation of more highly oxygenated compounds, dimers, oligomers, and other accretion products. Such condensed-phase reaction products with high molecular mass and low volatility can influence particle composition, viscosity, and diffusivity without being reflected in gas-phase measurements of condensable organic vapor concentrations and volatility distributions (Mehra et al., 2020; Maben and Ziemann, 2023; Kenseth et al., 2023; Kang et al., 2026).

Our model currently assigns identical self-diffusion coefficients to the many different organic compounds lumped into each bin of the applied decadic volatility basis sets (VBS). We note, however, that molecules in the same VBS bin may exhibit different properties such as diffusivity and desorption lifetime based on their molecular structure and functionalities, even if they exhibit similar intrinsic volatilities. Furthermore, the properties of organic aerosol mixtures may deviate from linear combinations of individual species properties. Fully resolving SOA nanoparticle growth may thus require a detailed accounting of matrix interactions, molecular identities and molecular corridors along which the gas-phase and condensed-phase composition of organic aerosols evolve (Shiraiwa et al., 2014; Li et al., 2016; Knopf et al., 2024).

Figure 3 shows a wide range of atmospheric nanoparticle growth rates plotted against organic vapor concentrations as observed in the Asian megacity of Beijing (China, Qiao et al., 2021), at the Europe rural background site San Pietro di Capofiume

(Italy, Cai et al., 2024), and at the boreal forest site Hyytiälä (Finland, Gonzalez Carracedo et al., 2022) alongside the CERN CLOUD chamber data as presented by Stolzenburg et al. (2025). Similar to the chamber experiments (circular markers), the field measurement data (diamond markers) exhibit a pronounced increase of OOMs concentrations with increasing temperature (color coding), which can be attributed to general trends of temperature-related enhancements in emissions of volatile organic compounds (VOC) as SOA precursors and photochemical reactivity leading to higher OOMs production rates in the atmosphere (Seinfeld and Pandis, 2016; Paasonen et al., 2018; Bianchi et al., 2019). While the OOMs concentrations vary by three orders of magnitude, the nanoparticle growth rates observed in the atmosphere remain rather uniformly confined to a narrow range around 1 to 10 nm h^{-1}.

The field measurement data points and their weak dependence on ambient temperature and measured OOMs concentration do not follow the kinetic-limit line (black dashed) to which they had been related in the recent study of Stolzenburg et al. (2025) highlighting incomplete mass closure of atmospheric nanoparticle growth. In contrast, the solid black fit line to our model results illustrates the weak apparent dependence on OOMs concentration which we obtain using KM3C to predict SOA nanoparticle growth rates as a function of temperature and organic vapor concentration assuming the same volatility distributions as observed in the CERN CLOUD experiments (square markers). The grey shaded areas in Fig. 3 illustrate that most of the growth rates observed in the field measurements and laboratory experiments reported by Stolzenburg et al. (2025) fall within a factor of three relative to this line.

The tilt and flattening of the high OOMs concentration dependence by kinetic-limit lines introduced in earlier studies (Stolzenburg et al., 2018, 2025) towards the weak OOMs concentration dependence indicated by KM3C can be attributed to the following key factors: (I) at low temperature and concentration levels, organic vapors that would have relatively high volatility at room temperature can also contribute to nanoparticle growth (upward shift indicated by the arrow on the left side of Figs. 3a,b); and (II) at high temperature and concentration levels, enhanced volatility, low diffusivity, slow surface-to-bulk transport, and differential concentration gradients decelerate the uptake of organic vapors and delay the equilibration of gas-particle partitioning (downward shift indicated by the arrow on the right side of Figs. 3a,b).

Overall, the variability and temperature dependencies of condensable organic vapor (OOMs) production by VOC oxidation, volatility, and diffusivity are partly offsetting and balancing each other. This balancing leads to an effective buffering of the vapor concentration dependence of atmospheric nanoparticle growth rates around 1 to 10 nm h^{-1} as observed and reported in earlier studies (Kulmala et al., 2004; Kulmala and Kerminen, 2008; Stolzenburg et al., 2023, 2025).

3 Conclusions and Outlook

This study provides an answer to the long-standing and enigmatic scientific question why atmospheric nanoparticle growth rates are fairly uniform under widely different ambient conditions and exhibit a low dependence on organic vapor concentration (OOMs). We have developed and applied a new kinetic multilayer model of multiphase chemistry (KM3C) to explain and reconcile discrepancies between field observations, laboratory experiments, theoretical considerations, and earlier model pre-

dictions by resolving the interplay and counteracting effects of temperature-dependent multiphase chemical reactivity, volatility, and diffusivity.

As illustrated in Fig. 4, we identified key factors that lead to an effective buffering and convergence of atmospheric nanoparticle growth rates around 1-10 nm h^{-1} in spite of highly variable ambient conditions, including temperature and organic vapor concentrations. The emission and oxidation of organic compounds that serve as SOA precursors, and the production and concentration of potentially condensable organic vapors in the atmosphere generally tend to increase with increasing temperature. At the same time, however, increasing temperature enhances the volatility and equilibrium vapor pressure of organic compounds, thus reducing the proportions of organic compounds that are actually available to condense under equilibrium conditions in accordance with the Clausius-Clapeyron equation (left side of Fig. 4).

Depending on temperature, chemical composition, and size, aerosol particles can adopt a variety of liquid, semi-solid, or solid phase states with widely varying viscosities and diffusivities. Diffusivity can be related to the intrinsic volatility of the condensable organic vapors. Increasing proportions of molecules with lower intrinsic volatility can thus increase the viscosity and reduce the diffusivity of organic aerosols at higher temperatures. Low diffusivity in highly viscous, semi-solid or solid particles can decelerate and kinetically limit the uptake and surface-to-bulk transport of organic vapor molecules, generate differential concentration gradients of compounds with different volatilities in the particle, and delay the equilibration of gas-particle partitioning (right side of Fig. 4). This kinetic limitation can inhibit and effectively buffer particle growth especially at high organic vapor concentration.

The combination and interplay of these effects can explain the previously enigmatic observation of similar growth rates in nanoparticle growth events with vastly different organic vapor concentrations as observed in well-defined laboratory experiments and ambient air around the world. To reproduce the measurement results from the nanoparticle growth events investigated in this study, we did not have to invoke chemical reactions in the condensed phase or at the surface of the particles as suggested in related earlier studies (Heitto et al., 2022; Stolzenburg et al., 2025). Nevertheless, such multiphase chemical reactions - in particular the formation of dimers and oligomers - may also influence the volatility distribution and particle diffusivity, and can be flexibly included in KM3C (Mehra et al., 2020; Berkemeier et al., 2020; Schervish et al., 2026; Kang et al., 2026). Another process affecting nanoparticle growth is coagulation, which can increase measured growth rates (Cai et al., 2021, 2026). Coagulation was not explicitly treated in this study, as Stolzenburg et al. (2025) reported little influence of coagulation for the investigated field data, while Stolzenburg et al. (2018) included it into their uncertainty estimates for the investigated chamber data. Moreover, the analysis and description of nanoparticle growth rates in atmospheric air masses can be influenced by differences between Lagrangian and Eulerian perspectives in the analysis and modeling of condensable vapor concentrations and aerosol particle size distributions. Such effects were not taken into account here but will be investigated in follow-up studies combining KM3C with regional and global 3D models of atmospheric transport and chemistry.

Our results show how composition- and temperature-dependent particle properties such as molecular diffusivity can influence and buffer the kinetics of gas-particle partitioning and the growth rates of nanoparticles. To further constrain key parameters and enhance the mechanistic understanding and predictability of nanoparticle growth under varying atmospheric conditions, we suggest to perform further laboratory experiments and field observations in which particle phase state and

diffusivity are determined alongside condensable vapor concentrations. Besides capturing the volatility distribution of all potentially condensable vapors, it will be important for future work to unravel the distribution and gradients of different organic compounds between and within particles across the relevant size range. For example, it may be possible to detect or infer radial concentration gradients in highly viscous particles (Huisman et al., 2025; Kang et al., 2026; Schervish et al., 2026) or detect deviations from the composition expected for the uninhibited growth of well-mixed, quasi-liquid particles (Lopez et al., 2025; Bhattacharyya et al., 2025). Kinetic process models, machine learning tools, and targeted uncertainty analysis combined in a numerical compass approach can aid the experimental design and help identify the experimental conditions that promise the largest gain of mechanistic understanding (Krüger et al., 2024). To achieve a full mechanistic and predictive understanding of atmospheric nanoparticle growth, we suggest and intend to further pursue and elaborate the integrative approach of data analysis and numerical modeling developed in this study, which has enabled the reconciliation of previously unexplained discrepancies between field observations and laboratory experiments, and theoretical considerations.

Code and data availability. The measurement data were adopted from Stolzenburg et al. (2018) and Stolzenburg et al. (2025). The KM3C model code is in preparation for public release as open source code.

Author contributions. TB and UP conceived the study. TB designed and supervised research. ZZ, HGK and TB built the kinetic model. ZZ performed kinetic model simulations and processed results. All authors analyzed and discussed the results, and co-wrote the paper led by TB and UP.

Competing interests. At least one of the (co-)authors is a member of the editorial board of ACP.

Acknowledgements. This work was funded by the Max Planck Society (MPG). HGK is supported by the Max Planck Graduate Center with the Johannes Gutenberg University Mainz (MPGC). The authors thank the Max Planck Computing and Data Facility (MPCDF) for computing time on the supercomputer RAVEN. We thank A. Mishra, M. Radecka, and colleagues across the scientific community for helpful discussions.

References

Antossian, C., Müller, M., and Krieger, U. K.: Photochemical and ozone-induced aging significantly alter the viscosity of aqueous *trans*-aconitic acid aerosol particles, Atmos. Chem. Phys., 26, 2443–2463, https://doi.org/10.5194/acp-26-2443-2026, 2026.

Arangio, A. M., Slade, J. H., Berkemeier, T., Pöschl, U., Knopf, D. A., and Shiraiwa, M.: Multiphase Chemical Kinetics of OH Radical Uptake by Molecular Organic Markers of Biomass Burning Aerosols: Humidity and Temperature Dependence, Surface Reaction, and Bulk Diffusion, J. Phys. Chem. A, 119, 4533–4544, https://doi.org/10.1021/jp510489z, 2015.

Artaxo, P., Hansson, H.-C., Andreae, M. O., Bäck, J., Alves, E. G., Barbosa, H. M. J., Bender, F., Bourtsoukidis, E., Carbone, S., Chi, J., Decesari, S., Després, V. R., Ditas, F., Ezhova, E., Fuzzi, S., Hasselquist, N. J., Heintzenberg, J., Holanda, B. A., Guenther, A., Hakola, H., Heikkinen, L., Kerminen, V.-M., Kontkanen, J., Krejci, R., Kulmala, M., Lavric, J. V., de Leeuw, G., Lehtipalo, K., Machado, L. A. T., McFiggans, G., Franco, M. A. M., Meller, B. B., Morais, F. G., Mohr, C., Morgan, W., Nilsson, M. B., Peichl, M., Petäjä, T., Praß, M., Pöhlker, C., Pöhlker, M. L., Pöschl, U., Von Randow, C., Riipinen, I., Rinne, J., Rizzo, L. V., Rosenfeld, D., Silva Dias, M. A. F., Sogacheva, L., Stier, P., Swietlicki, E., Sörgel, M., Tunved, P., Virkkula, A., Wang, J., Weber, B., Yáñez-Serrano, A. M., Zieger, P., Mikhailov, E., Smith, J. N., and Kesselmeier, J.: Tropical and Boreal Forest – Atmosphere Interactions: A Review, Tellus B: Chem. Phys. Meteorol., https://doi.org/10.16993/tellusb.34, 2022.

Bateman, A. P., Gong, Z., Liu, P., Sato, B., Cirino, G., Zhang, Y., Artaxo, P., Bertram, A. K., Manzi, A. O., Rizzo, L. V., Souza, R. A. F., Zaveri, R. A., and Martin, S. T.: Sub-micrometre particulate matter is primarily in liquid form over Amazon rainforest, Nat. Geosci., 9, 34–37, https://doi.org/10.1038/ngeo2599, 2016.

Berkemeier, T., Huisman, A. J., Ammann, M., Shiraiwa, M., Koop, T., and Pöschl, U.: Kinetic regimes and limiting cases of gas uptake and heterogeneous reactions in atmospheric aerosols and clouds: a general classification scheme, Atmos. Chem. Phys., 13, 6663–6686, https://doi.org/10.5194/acp-13-6663-2013, 2013.

Berkemeier, T., Shiraiwa, M., Pöschl, U., and Koop, T.: Competition between water uptake and ice nucleation by glassy organic aerosol particles, Atmos. Chem. Phys., 14, 12 513–12 531, https://doi.org/10.5194/acp-14-12513-2014, 2014.

Berkemeier, T., Steimer, S. S., Krieger, U. K., Peter, T., Pöschl, U., Ammann, M., and Shiraiwa, M.: Ozone uptake on glassy, semi-solid and liquid organic matter and the role of reactive oxygen intermediates in atmospheric aerosol chemistry, Phys. Chem. Chem. Phys., 18, 12 662–12 674, https://doi.org/10.1039/C6CP00634E, 2016.

Berkemeier, T., Takeuchi, M., Eris, G., and Ng, N. L.: Kinetic modeling of formation and evaporation of secondary organic aerosol from NO_3 oxidation of pure and mixed monoterpenes, Atmos. Chem. Phys., 20, 15 513–15 535, https://doi.org/10.5194/acp-20-15513-2020, 2020.

Bhattacharyya, N., Lopez, B., DeVivo, J., Russell, D. M., Shen, J., Sommer, E., Almeida, J., Amorim, A., Beckmann, H. M., Busato, M., Canagaratna, M. R., Caudillo, L., Chassaing, A., Christoudias, T., Dada, L., El-Haddad, I., Flagan, R. C., Harder, H., Judmaier, B., Kaniyodical Sebastian, M., Kirkby, J., Klebach, H., Kulmala, M., Kunkler, F., Lehtipalo, K., Liu, L., Mentler, B., Möhler, O., Morawiec, A., Petäjä, T., Rato, P., Rörup, B., Ruhl, S., Scholz, W., Simon, M., Tóme, A., Tong, Y., Top, J., Umo, N. S., Volkamer, R., Weissbacher, J., Worsnop, D. R., Xenofontos, C., Yang, B., Yu, W., Zauner-Wieczorek, M., Zgheib, I., Zhang, J., Zheng, Z., He, X.-C., Stolzenburg, D., Schobesberger, S., Curtius, J., and Donahue, N. M.: Isoprene Aerosol Growth in the Upper Troposphere: Application of the Diagonal Volatility Basis Set to CLOUD Chamber Measurements, ACS ES&T Air, 2, 2092–2104, https://doi.org/10.1021/acsestair.5c00106, 2025.

Bianchi, F., Tröstl, J., Junninen, H., Frege, C., Henne, S., Hoyle, C. R., Molteni, U., Herrmann, E., Adamov, A., Bukowiecki, N., Chen, X., Duplissy, J., Gysel, M., Hutterli, M., Kangasluoma, J., Kontkanen, J., Kürten, A., Manninen, H. E., Münch, S., Peräkylä, O., Petäjä, T., Rondo, L., Williamson, C., Weingartner, E., Curtius, J., Worsnop, D. R., Kulmala, M., Dommen, J., and Baltensperger, U.: New particle

formation in the free troposphere: A question of chemistry and timing, Science, 352, 1109–1112, https://doi.org/10.1126/science.aad5456, 2016.

Bianchi, F., Kurtén, T., Riva, M., Mohr, C., Rissanen, M. P., Roldin, P., Berndt, T., Crounse, J. D., Wennberg, P. O., Mentel, T. F., Wildt, J., Junninen, H., Jokinen, T., Kulmala, M., Worsnop, D. R., Thornton, J. A., Donahue, N., Kjaergaard, H. G., and Ehn, M.: Highly Oxygenated Organic Molecules (HOM) from Gas-Phase Autoxidation Involving Peroxy Radicals: A Key Contributor to Atmospheric Aerosol, Chem. Rev., 119, 3472–3509, https://doi.org/10.1021/acs.chemrev.8b00395, 2019.

Bilde, M., Barsanti, K., Booth, M., Cappa, C. D., Donahue, N. M., Emanuelsson, E. U., McFiggans, G., Krieger, U. K., Marcolli, C., Topping, D., Ziemann, P., Barley, M., Clegg, S., Dennis-Smither, B., Hallquist, M., Hallquist, M., Khlystov, A., Kulmala, M., Mogensen, D., Percival, C. J., Pope, F., Reid, J. P., Ribeiro da Silva, M. A. V., Rosenoern, T., Salo, K., Soonsin, V. P., Yli-Juuti, T., Prisle, N. L., Pagels, J., Rarey, J., Zardini, A. A., and Riipinen, I.: Saturation Vapor Pressures and Transition Enthalpies of Low-Volatility Organic Molecules of Atmospheric Relevance: From Dicarboxylic Acids to Complex Mixtures, Chem. Rev., 115, 4115–4156, https://doi.org/10.1021/cr5005502, 2015.

Cai, J., Sulo, J., Gu, Y., Holm, S., Cai, R., Thomas, S., Neuberger, A., Mattsson, F., Paglione, M., Decesari, S., Rinaldi, M., Yin, R., Aliaga, D., Huang, W., Li, Y., Gramlich, Y., Ciarelli, G., Quéléver, L., Sarnela, N., Lehtipalo, K., Zannoni, N., Wu, C., Nie, W., Kangasluoma, J., Mohr, C., Kulmala, M., Zha, Q., Stolzenburg, D., and Bianchi, F.: Elucidating the mechanisms of atmospheric new particle formation in the highly polluted Po Valley, Italy, Atmos. Chem. Phys., 24, 2423–2441, https://doi.org/10.5194/acp-24-2423-2024, 2024.

Cai, R., Li, C., He, X.-C., Deng, C., Lu, Y., Yin, R., Yan, C., Wang, L., Jiang, J., Kulmala, M., and Kangasluoma, J.: Impacts of coagulation on the appearance time method for new particle growth rate evaluation and their corrections, Atmos. Chem. Phys., 21, 2287–2304, https://doi.org/10.5194/acp-21-2287-2021, 2021.

Cai, R., Li, X., Li, Y., Blichner, S., Stolzenburg, D., Zha, Q., Cai, J., Nie, W., Yan, C., Huang, D. D., Wang, Z., Wu, J., Yin, R., Sarnela, N., Huang, W., Tuovinen, S., Holm, S., Ahonen, L., Yao, L., Ding, A., Bianchi, F., Liu, Y., Winkler, P. M., Petäjä, T., Chen, J., Kerminen, V.-M., Wang, L., Worsnop, D., Jiang, J., Kulmala, M., and Kangasluoma, J.: The key role of nanoparticle concentration gradient in aerosol initial growth, Nat. Commun., https://doi.org/10.1038/s41467-026-70082-2, 2026.

Cheng, Y., Su, H., Koop, T., Mikhailov, E., and Pöschl, U.: Size dependence of phase transitions in aerosol nanoparticles, Nat. Commun., 6, 5923, https://doi.org/10.1038/ncomms6923, 2015.

Dada, L., Stolzenburg, D., Simon, M., Fischer, L., Heinritzi, M., Wang, M., Xiao, M., Vogel, A. L., Ahonen, L., Amorim, A., Baalbaki, R., Baccarini, A., Baltensperger, U., Bianchi, F., Daellenbach, K. R., DeVivo, J., Dias, A., Dommen, J., Duplissy, J., Finkenzeller, H., Hansel, A., He, X.-C., Hofbauer, V., Hoyle, C. R., Kangasluoma, J., Kim, C., Kürten, A., Kvashnin, A., Mauldin, R., Makhmutov, V., Marten, R., Mentler, B., Nie, W., Petäjä, T., Quéléver, L. L. J., Saathoff, H., Tauber, C., Tome, A., Molteni, U., Volkamer, R., Wagner, R., Wagner, A. C., Wimmer, D., Winkler, P. M., Yan, C., Zha, Q., Rissanen, M., Gordon, H., Curtius, J., Worsnop, D. R., Lehtipalo, K., Donahue, N. M., Kirkby, J., El Haddad, I., and Kulmala, M.: Role of sesquiterpenes in biogenic new particle formation, Sci. Adv., 9, https://doi.org/10.1126/sciadv.adi5297, 2023.

Dette, H. P. and Koop, T.: Glass Formation Processes in Mixed Inorganic/Organic Aerosol Particles, J. Phys. Chem. A, 119, 4552–4561, https://doi.org/10.1021/jp5106967, 2015.

Donahue, N. M., Robinson, A. L., Stanier, C. O., and Pandis, S. N.: Coupled Partitioning, Dilution, and Chemical Aging of Semivolatile Organics, Environ. Sci. Technol., 40, 2635–2643, https://doi.org/10.1021/es052297c, 2006.

Donahue, N. M., Epstein, S. A., Pandis, S. N., and Robinson, A. L.: A two-dimensional volatility basis set: 1. organic-aerosol mixing thermodynamics, Atmos. Chem. Phys., 11, 3303–3318, https://doi.org/10.5194/acp-11-3303-2011, 2011.

Donahue, N. M., Dada, L., Stolzenburg, D., Sommer, E., Simon, M., Schervish, M., DeVivo, J., Stinchfield, A., Burton, N., Bhattacharyya, N., Lopez, B., Wang, M., Scholz, W., Almeida, J., Zhao, B., Heinritzi, M., Gordon, H., Hansel, A., Curtius, J., Lehtipalo, K., El Haddad, I., Kirkby, J., Flagan, R., Kulmala, M., and Worsnop, D.: On describing particle nucleation within the Volatility Basis Set, Atmos. Chem. Phys., 26, 8311–8339, https://doi.org/10.5194/acp-26-8311-2026, 2026.

Epstein, S. A., Riipinen, I., and Donahue, N. M.: A Semiempirical Correlation between Enthalpy of Vaporization and Saturation Concentration for Organic Aerosol, Environ. Sci. Technol., 44, 743–748, https://doi.org/10.1021/es902497z, pMID: 20025284, 2010.

Golay, Z. M., Vandergrift, G. W., Kamal, S., China, S., Nizkorodov, S. A., and Bertram, A. K.: Sunlight can turn smoldering pine wood smoke into a glass, npj Clean Air, 2, 29, https://doi.org/10.1038/s44407-026-00070-9, 2026.

Gonzalez Carracedo, L., Lehtipalo, K., Ahonen, L. R., Sarnela, N., Holm, S., Kangasluoma, J., Kulmala, M., Winkler, P. M., and Stolzenburg, D.: On the relation between apparent ion and total particle growth rates in the boreal forest and related chamber experiments, Atmos. Chem. Phys., 22, 13 153–13 166, https://doi.org/10.5194/acp-22-13153-2022, 2022.

Gordon, H., Kirkby, J., Baltensperger, U., Bianchi, F., Breitenlechner, M., Curtius, J., Dias, A., Dommen, J., Donahue, N. M., Dunne, E. M., Duplissy, J., Ehrhart, S., Flagan, R. C., Frege, C., Fuchs, C., Hansel, A., Hoyle, C. R., Kulmala, M., Kürten, A., Lehtipalo, K., Makhmutov, V., Molteni, U., Rissanen, M. P., Stozkhov, Y., Tröstl, J., Tsagkogeorgas, G., Wagner, R., Williamson, C., Wimmer, D., Winkler, P. M., Yan, C., and Carslaw, K. S.: Causes and importance of new particle formation in the present-day and preindustrial atmospheres, J. Geophys. Res.: Atmos., 122, 8739–8760, https://doi.org/10.1002/2017jd026844, 2017.

Hallquist, M., Wenger, J. C., Baltensperger, U., Rudich, Y., Simpson, D., Claeys, M., Dommen, J., Donahue, N. M., George, C., Goldstein, A. H., Hamilton, J. F., Herrmann, H., Hoffmann, T., Iinuma, Y., Jang, M., Jenkin, M. E., Jimenez, J. L., Kiendler-Scharr, A., Maenhaut, W., McFiggans, G., Mentel, T. F., Monod, A., Prévôt, A. S. H., Seinfeld, J. H., Surratt, J. D., Szmigielski, R., and Wildt, J.: The formation, properties and impact of secondary organic aerosol: current and emerging issues, Atmos. Chem. Phys., 9, 5155–5236, https://doi.org/10.5194/acp-9-5155-2009, 2009.

Heitto, A., Lehtinen, K., Petäjä, T., Lopez-Hilfiker, F., Thornton, J. A., Kulmala, M., and Yli-Juuti, T.: Effects of oligomerization and decomposition on the nanoparticle growth: a model study, Atmos. Chem. Phys., 22, 155–171, https://doi.org/10.5194/acp-22-155-2022, 2022.

Hellén, H., Praplan, A. P., Tykkä, T., Ylivinkka, I., Vakkari, V., Bäck, J., Petäjä, T., Kulmala, M., and Hakola, H.: Long-term measurements of volatile organic compounds highlight the importance of sesquiterpenes for the atmospheric chemistry of a boreal forest, Atmos. Chem. Phys., 18, 13 839–13 863, https://doi.org/10.5194/acp-18-13839-2018, 2018.

Huisman, M., Poon, W. C. K., Warren, P. B., Titmuss, S., and Marenduzzo, D.: Diffusive evaporation dynamics in polymer solutions is ubiquitous, Soft Matter, 21, 1508–1515, https://doi.org/10.1039/D4SM01215A, 2025.

IPCC: Climate Change 2023: Synthesis Report. Contribution of Working Groups I, II and III to the Sixth Assessment Report of the Intergovernmental Panel on Climate Change, https://doi.org/10.59327/IPCC/AR6-9789291691647, 2023.

Jimenez, J. L., Canagaratna, M. R., Donahue, N. M., Prevot, A. S. H., Zhang, Q., Kroll, J. H., DeCarlo, P. F., Allan, J. D., Coe, H., Ng, N. L., Aiken, A. C., Docherty, K. S., Ulbrich, I. M., Grieshop, A. P., Robinson, A. L., Duplissy, J., Smith, J. D., Wilson, K. R., Lanz, V. A., Hueglin, C., Sun, Y. L., Tian, J., Laaksonen, A., Raatikainen, T., Rautiainen, J., Vaattovaara, P., Ehn, M., Kulmala, M., Tomlinson, J. M., Collins, D. R., Cubison, M. J., Dunlea, J., Huffman, J. A., Onasch, T. B., Alfarra, M. R., Williams, P. I., Bower, K., Kondo, Y., Schneider, J., Drewnick, F., Borrmann, S., Weimer, S., Demerjian, K., Salcedo, D., Cottrell, L., Griffin, R., Takami, A., Miyoshi, T., Hatakeyama, S., Shimono, A., Sun, J. Y., Zhang, Y. M., Dzepina, K., Kimmel, J. R., Sueper, D., Jayne, J. T., Herndon, S. C., Trimborn, A. M., Williams,

L. R., Wood, E. C., Middlebrook, A. M., Kolb, C. E., Baltensperger, U., and Worsnop, D. R.: Evolution of Organic Aerosols in the Atmosphere, Science, 326, 1525–1529, https://doi.org/10.1126/science.1180353, 2009.

Kang, H. G., Takeuchi, M., Ng, N. L., Pöschl, U., and Berkemeier, T.: Multiphase Chemistry and Phase State Explain Nonlinear Effects in the Formation and Evaporation of SOA from Mixed Monoterpene Precursors, ACS ES&T Air, https://doi.org/10.1021/acsestair.5c00438, 2026.

Kenseth, C. M., Hafeman, N. J., Rezgui, S. P., Chen, J., Huang, Y., Dalleska, N. F., Kjaergaard, H. G., Stoltz, B. M., Seinfeld, J. H., and Wennberg, P. O.: Particle-phase accretion forms dimer esters in pinene secondary organic aerosol, Science, 382, 787–792, https://doi.org/10.1126/science.adi0857, 2023.

Kiland, K. J., Maclean, A. M., Kamal, S., and Bertram, A. K.: Diffusion of Organic Molecules as a Function of Temperature in a Sucrose Matrix (a Proxy for Secondary Organic Aerosol), J. Phys. Chem. Lett., 10, 5902–5908, https://doi.org/10.1021/acs.jpclett.9b02182, 2019.

Knopf, D. A., Ammann, M., Berkemeier, T., Pöschl, U., and Shiraiwa, M.: Desorption lifetimes and activation energies influencing gas–surface interactions and multiphase chemical kinetics, Atmos. Chem. Phys., 24, 3445–3528, https://doi.org/10.5194/acp-24-3445-2024, 2024.

Koop, T., Bookhold, J., Shiraiwa, M., and Pöschl, U.: Glass transition and phase state of organic compounds: dependency on molecular properties and implications for secondary organic aerosols in the atmosphere, Phys. Chem. Chem. Phys., 13, 19 238, https://doi.org/10.1039/c1cp22617g, 2011.

Krüger, M., Mishra, A., Spichtinger, P., Pöschl, U., and Berkemeier, T.: A numerical compass for experiment design in chemical kinetics and molecular property estimation, J. Cheminf., 16, 34, https://doi.org/10.1186/s13321-024-00825-0, 2024.

Kulmala, M. and Kerminen, V.-M.: On the formation and growth of atmospheric nanoparticles, Atmos. Res., 90, 132–150, https://doi.org/https://doi.org/10.1016/j.atmosres.2008.01.005, 2008.

Kulmala, M., Vehkamäki, H., Petäjä, T., Dal Maso, M., Lauri, A., Kerminen, V.-M., Birmili, W., and McMurry, P.: Formation and growth rates of ultrafine atmospheric particles: a review of observations, J. Aerosol Sci., 35, 143–176, https://doi.org/10.1016/j.jaerosci.2003.10.003, 2004.

Kulmala, M., Petäjä, T., Ehn, M., Thornton, J., Sipilä, M., Worsnop, D., and Kerminen, V.-M.: Chemistry of Atmospheric Nucleation: On the Recent Advances on Precursor Characterization and Atmospheric Cluster Composition in Connection with Atmospheric New Particle Formation, Annu. Rev. Phys. Chem., 65, 21–37, https://doi.org/10.1146/annurev-physchem-040412-110014, 2014.

Kulmala, M., Cai, R., Stolzenburg, D., Zhou, Y., Dada, L., Guo, Y., Yan, C., Petäjä, T., Jiang, J., and Kerminen, V.-M.: The contribution of new particle formation and subsequent growth to haze formation, Environ. Sci.: Atmos., 2, 352–361, https://doi.org/10.1039/D1EA00096A, 2022.

Li, Y., Pöschl, U., and Shiraiwa, M.: Molecular corridors and parameterizations of volatility in the chemical evolution of organic aerosols, Atmos. Chem. Phys., 16, 3327–3344, https://doi.org/10.5194/acp-16-3327-2016, 2016.

Li, Y., Day, D. A., Stark, H., Jimenez, J. L., and Shiraiwa, M.: Predictions of the glass transition temperature and viscosity of organic aerosols from volatility distributions, Atmos. Chem. Phys., 20, 8103–8122, https://doi.org/10.5194/acp-20-8103-2020, 2020.

Lopez, B., Bhattacharyya, N., DeVivo, J., Wang, M., Caudillo-Plath, L., Surdu, M., Bianchi, F., Brasseur, Z., Buchholz, A., Chen, D., Duplissy, J., He, X.-C., Hofbauer, V., Mahfouz, N., Makhmutov, V., Marten, R., Mentler, B., Philippov, M., Schervish, M., Wang, D. S., Weber, S. K., Welti, A., El Haddad, I., Lehtipalo, K., Kulmala, M., Worsnop, D., Kirkby, J., Mauldin, R. L., Stolzenburg, D., Schobesberger, S., Flagan, R., and Donahue, N. M.: A diagonal volatility basis set to assess the condensation of organic vapors onto particles, Environ. Sci.: Atmos., 5, 1035–1061, https://doi.org/10.1039/d5ea00062a, 2025.

Maben, H. K. and Ziemann, P. J.: Kinetics of oligomer-forming reactions involving the major functional groups present in atmospheric secondary organic aerosol particles, Environ. Sci.: Processes Impacts, 25, 214–228, https://doi.org/10.1039/D2EM00124A, 2023.

Mahant, S., Snider, J. R., Petters, S. S., and Petters, M. D.: Effect of Aerosol Size on Glass Transition Temperature, J. Phys. Chem. Lett., 15, 7509–7515, https://doi.org/10.1021/acs.jpclett.4c01415, 2024.

McNeill, V. F., Loerting, T., Geiger, F. M., Trout, B. L., and Molina, M. J.: Hydrogen chloride-induced surface disordering on ice, P. Natl. Acad. Sci. USA, 103, 9422–9427, https://doi.org/10.1073/pnas.0603494103, 2006.

Mehra, A., Krechmer, J. E., Lambe, A., Sarkar, C., Williams, L., Khalaj, F., Guenther, A., Jayne, J., Coe, H., Worsnop, D., Faiola, C., and Canagaratna, M.: Oligomer and highly oxygenated organic molecule formation from oxidation of oxygenated monoterpenes emitted by California sage plants, Atmos. Chem. Phys., 20, 10 953–10 965, https://doi.org/10.5194/acp-20-10953-2020, 2020.

Mikhailov, E., Vlasenko, S., Martin, S. T., Koop, T., and Pöschl, U.: Amorphous and crystalline aerosol particles interacting with water vapor: conceptual framework and experimental evidence for restructuring, phase transitions and kinetic limitations, Atmos. Chem. Phys., 9, 9491–9522, https://doi.org/10.5194/acp-9-9491-2009, 2009.

Mohr, C., Thornton, J. A., Heitto, A., Lopez-Hilfiker, F. D., Lutz, A., Riipinen, I., Hong, J., Donahue, N. M., Hallquist, M., Petäjä, T., Kulmala, M., and Yli-Juuti, T.: Molecular identification of organic vapors driving atmospheric nanoparticle growth, Nat. Commun., 10, https://doi.org/10.1038/s41467-019-12473-2, 2019.

Mu, Q., Shiraiwa, M., Octaviani, M., Ma, N., Ding, A., Su, H., Lammel, G., Pöschl, U., and Cheng, Y.: Temperature effect on phase state and reactivity controls atmospheric multiphase chemistry and transport of PAHs, Sci. Adv., 4, eaap7314, https://doi.org/10.1126/sciadv.aap7314, 2018.

Paasonen, P., Peltola, M., Kontkanen, J., Junninen, H., Kerminen, V.-M., and Kulmala, M.: Comprehensive analysis of particle growth rates from nucleation mode to cloud condensation nuclei in boreal forest, Atmos. Chem. Phys., 18, 12 085–12 103, https://doi.org/10.5194/acp-18-12085-2018, 2018.

Pfrang, C., Shiraiwa, M., and Pöschl, U.: Chemical ageing and transformation of diffusivity in semi-solid multi-component organic aerosol particles, Atmos. Chem. Phys., 11, 7343–7354, https://doi.org/10.5194/acp-11-7343-2011, 2011.

Qiao, X., Yan, C., Li, X., Guo, Y., Yin, R., Deng, C., Li, C., Nie, W., Wang, M., Cai, R., Huang, D., Wang, Z., Yao, L., Worsnop, D. R., Bianchi, F., Liu, Y., Donahue, N. M., Kulmala, M., and Jiang, J.: Contribution of Atmospheric Oxygenated Organic Compounds to Particle Growth in an Urban Environment, Environ. Sci. Technol., 55, 13 646–13 656, https://doi.org/10.1021/acs.est.1c02095, 2021.

Reid, J. P., Bertram, A. K., Topping, D. O., Laskin, A., Martin, S. T., Petters, M. D., Pope, F. D., and Rovelli, G.: The viscosity of atmospherically relevant organic particles, Nat. Commun., 9, 956, https://doi.org/10.1038/s41467-018-03027-z, 2018.

Renbaum-Wolff, L., Grayson, J. W., Bateman, A. P., Kuwata, M., Sellier, M., Murray, B. J., Shilling, J. E., Martin, S. T., and Bertram, A. K.: Viscosity of α-pinene secondary organic material and implications for particle growth and reactivity, P. Natl. Acad. Sci. USA, 110, 8014–8019, https://doi.org/10.1073/pnas.1219548110, 2013.

Riipinen, I., Pierce, J. R., Yli-Juuti, T., Nieminen, T., Häkkinen, S., Ehn, M., Junninen, H., Lehtipalo, K., Petäjä, T., Slowik, J., Chang, R., Shantz, N. C., Abbatt, J., Leaitch, W. R., Kerminen, V.-M., Worsnop, D. R., Pandis, S. N., Donahue, N. M., and Kulmala, M.: Organic condensation: a vital link connecting aerosol formation to cloud condensation nuclei (CCN) concentrations, Atmos. Chem. Phys., 11, 3865–3878, https://doi.org/10.5194/acp-11-3865-2011, 2011.

Riva, M., Rantala, P., Krechmer, J. E., Peräkylä, O., Zhang, Y., Heikkinen, L., Garmash, O., Yan, C., Kulmala, M., Worsnop, D., and Ehn, M.: Evaluating the performance of five different chemical ionization techniques for detecting gaseous oxygenated organic species, Atmos. Meas. Tech., 12, 2403–2421, https://doi.org/10.5194/amt-12-2403-2019, 2019.

Saukko, E., Lambe, A. T., Massoli, P., Koop, T., Wright, J. P., Croasdale, D. R., Pedernera, D. A., Onasch, T. B., Laaksonen, A., Davidovits, P., Worsnop, D. R., and Virtanen, A.: Humidity-dependent phase state of SOA particles from biogenic and anthropogenic precursors, Atmos. Chem. Phys., 12, 7517–7529, https://doi.org/10.5194/acp-12-7517-2012, 2012.

Schervish, M. and Donahue, N. M.: Peroxy radical chemistry and the volatility basis set, Atmos. Chem. Phys., 20, 1183–1199, https://doi.org/10.5194/acp-20-1183-2020, 2020.

Schervish, M., Kang, H. G., Wingen, L. M., Nguyen, K., Begay, C., Wilson, J., Shrivastava, M., Chen, Y., Shilling, J. E., Ng, N. L., Pöschl, U., Berkemeier, T., Zelenyuk, A., and Shiraiwa, M.: Surface Crust Formation Controls Evaporation Kinetics of Secondary Organic Aerosols, Environ. Sci. Technol., 60, 7995–8006, https://doi.org/10.1021/acs.est.5c11018, 2026.

Seinfeld, J. H. and Pandis, S. N.: Atmospheric chemistry and physics: from air pollution to climate change, John Wiley & Sons, 2016.

Shiraiwa, M., Ammann, M., Koop, T., and Pöschl, U.: Gas uptake and chemical aging of semisolid organic aerosol particles, P. Natl. Acad. Sci. USA, 108, 11 003–11 008, https://doi.org/10.1073/pnas.1103045108, 2011.

Shiraiwa, M., Berkemeier, T., Schilling-Fahnestock, K. A., Seinfeld, J. H., and Pöschl, U.: Molecular corridors and kinetic regimes in the multiphase chemical evolution of secondary organic aerosol, Atmos. Chem. Phys., 14, 8323–8341, https://doi.org/10.5194/acp-14-8323-2014, 2014.

Shiraiwa, M., Li, Y., Tsimpidi, A. P., Karydis, V. A., Berkemeier, T., Pandis, S. N., Lelieveld, J., Koop, T., and Pöschl, U.: Global distribution of particle phase state in atmospheric secondary organic aerosols, Nat. Commun., 8, 15 002, https://doi.org/10.1038/ncomms15002, 2017.

Shrivastava, M., Cappa, C. D., Fan, J., Goldstein, A. H., Guenther, A. B., Jimenez, J. L., Kuang, C., Laskin, A., Martin, S. T., Ng, N. L., Petaja, T., Pierce, J. R., Rasch, P. J., Roldin, P., Seinfeld, J. H., Shilling, J., Smith, J. N., Thornton, J. A., Volkamer, R., Wang, J., Worsnop, D. R., Zaveri, R. A., Zelenyuk, A., and Zhang, Q.: Recent advances in understanding secondary organic aerosol: Implications for global climate forcing, Rev. Geophys., 55, 509–559, https://doi.org/10.1002/2016RG000540, 2017.

Slade, J. H., Ault, A. P., Bui, A. T., Ditto, J. C., Lei, Z., Bondy, A. L., Olson, N. E., Cook, R. D., Desrochers, S. J., Harvey, R. M., Erickson, M. H., Wallace, H. W., Alvarez, S. L., Flynn, J. H., Boor, B. E., Petrucci, G. A., Gentner, D. R., Griffin, R. J., and Shepson, P. B.: Bouncier Particles at Night: Biogenic Secondary Organic Aerosol Chemistry and Sulfate Drive Diel Variations in the Aerosol Phase in a Mixed Forest, Environ. Sci. Technol., 53, 4977–4987, https://doi.org/10.1021/acs.est.8b07319, pMID: 31002496, 2019.

Stevenson, J. D. and Wolynes, P. G.: On the surface of glasses, J. Chem. Phys., 129, 234 514, https://doi.org/10.1063/1.3041651, 2008.

Stolzenburg, D., Fischer, L., Vogel, A. L., Heinritzi, M., Schervish, M., Simon, M., Wagner, A. C., Dada, L., Ahonen, L. R., Amorim, A., Baccarini, A., Bauer, P. S., Baumgartner, B., Bergen, A., Bianchi, F., Breitenlechner, M., Brilke, S., Buenrostro Mazon, S., Chen, D., Dias, A., Draper, D. C., Duplissy, J., El Haddad, I., Finkenzeller, H., Frege, C., Fuchs, C., Garmash, O., Gordon, H., He, X., Helm, J., Hofbauer, V., Hoyle, C. R., Kim, C., Kirkby, J., Kontkanen, J., Kürten, A., Lampilahti, J., Lawler, M., Lehtipalo, K., Leiminger, M., Mai, H., Mathot, S., Mentler, B., Molteni, U., Nie, W., Nieminen, T., Nowak, J. B., Ojdanic, A., Onnela, A., Passananti, M., Petäjä, T., Quéléver, L. L. J., Rissanen, M. P., Sarnela, N., Schallhart, S., Tauber, C., Tomé, A., Wagner, R., Wang, M., Weitz, L., Wimmer, D., Xiao, M., Yan, C., Ye, P., Zha, Q., Baltensperger, U., Curtius, J., Dommen, J., Flagan, R. C., Kulmala, M., Smith, J. N., Worsnop, D. R., Hansel, A., Donahue, N. M., and Winkler, P. M.: Rapid growth of organic aerosol nanoparticles over a wide tropospheric temperature range, P. Natl. Acad. Sci. USA, 115, 9122–9127, https://doi.org/10.1073/pnas.1807604115, 2018.

Stolzenburg, D., Wang, M., Schervish, M., and Donahue, N. M.: Tutorial: Dynamic organic growth modeling with a volatility basis set, J. Aerosol Sci., 166, 106 063, https://doi.org/10.1016/j.jaerosci.2022.106063, 2022.

Stolzenburg, D., Cai, R., Blichner, S. M., Kontkanen, J., Zhou, P., Makkonen, R., Kerminen, V.-M., Kulmala, M., Riipinen, I., and Kangasluoma, J.: Atmospheric nanoparticle growth, Rev. Mod. Phys., 95, 045 002, https://doi.org/10.1103/RevModPhys.95.045002, 2023.

Stolzenburg, D., Sarnela, N., Bianchi, F., Cai, J., Cai, R., Cheng, Y., Dada, L., Donahue, N. M., Grothe, H., Holm, S., Kerminen, V.-M., Lehtipalo, K., Petäjä, T., Sulo, J., Winkler, P. M., Yan, C., Kangasluoma, J., and Kulmala, M.: Incomplete mass closure in atmospheric nanoparticle growth, npj Clim. Atmos. Sci., 8, https://doi.org/10.1038/s41612-025-00893-5, 2025.

Tian, H., Xu, Q., Zhang, H., Priestley, R. D., and Zuo, B.: Surface dynamics of glasses, Appl. Phys. Rev., 9, 011 316, https://doi.org/10.1063/5.0083726, 2022.

Virtanen, A., Joutsensaari, J., Koop, T., Kannosto, J., Yli-Pirilä, P., Leskinen, J., Mäkelä, J. M., Holopainen, J. K., Pöschl, U., Kulmala, M., Worsnop, D. R., and Laaksonen, A.: An amorphous solid state of biogenic secondary organic aerosol particles, Nature, 467, 824–827, https://doi.org/10.1038/nature09455, 2010.

WHO: Health workforce support and safeguards list 2023, Tech. rep., World Health Organization, Geneva, Switzerland, https://www.who.int/publications/i/item/9789240069787, accessed: 2026 April 1, 2023.

Yli-Juuti, T., Mohr, C., and Riipinen, I.: Open questions on atmospheric nanoparticle growth, Commun. Chem., 3, 106, https://doi.org/10.1038/s42004-020-00339-4, 2020.

Zaveri, R. A., Easter, R. C., Shilling, J. E., and Seinfeld, J. H.: Modeling kinetic partitioning of secondary organic aerosol and size distribution dynamics: representing effects of volatility, phase state, and particle-phase reaction, Atmos. Chem. Phys., 14, 5153–5181, https://doi.org/10.5194/acp-14-5153-2014, 2014.

Zaveri, R. A., Shilling, J. E., Zelenyuk, A., Liu, J., Bell, D. M., D'Ambro, E. L., Gaston, C. J., Thornton, J. A., Laskin, A., Lin, P., Wilson, J., Easter, R. C., Wang, J., Bertram, A. K., Martin, S. T., Seinfeld, J. H., and Worsnop, D. R.: Growth Kinetics and Size Distribution Dynamics of Viscous Secondary Organic Aerosol, Environ. Sci. Technol., 52, 1191–1199, https://doi.org/10.1021/acs.est.7b04623, 2018.

Zaveri, R. A., Shilling, J. E., Zelenyuk, A., Zawadowicz, M. A., Suski, K., China, S., Bell, D. M., Veghte, D., and Laskin, A.: Particle-Phase Diffusion Modulates Partitioning of Semivolatile Organic Compounds to Aged Secondary Organic Aerosol, Environ. Sci. Technol., 54, 2595–2605, https://doi.org/10.1021/acs.est.9b05514, 2020.

Zhou, S., Shiraiwa, M., McWhinney, R. D., Pöschl, U., and Abbatt, J. P. D.: Kinetic limitations in gas-particle reactions arising from slow diffusion in secondary organic aerosol, Faraday Discuss., 165, 391–406, https://doi.org/10.1039/C3FD00030C, 2013.

Zobrist, B., Marcolli, C., Pedernera, D. A., and Koop, T.: Do atmospheric aerosols form glasses?, Atmos. Chem. Phys., 8, 5221–5244, https://doi.org/10.5194/acp-8-5221-2008, 2008.

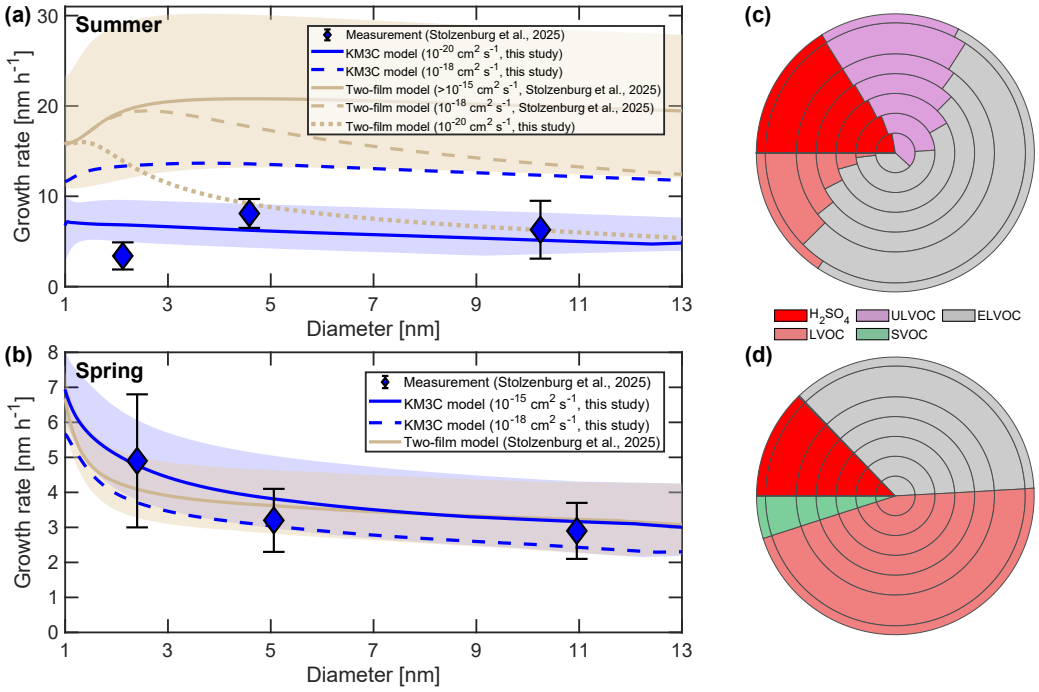

Figure 1. Atmospheric nanoparticle growth observed in field measurements. Blue diamond markers and error bars represent arithmetic mean values and standard deviations of growth rates measured in **(a)** summer and **(b)** spring at a boreal forest site (Hyytiälä, Finland; Gonzalez Carracedo et al. (2022)). Lines and shadings represent model predictions and uncertainty ranges obtained with a traditional two-film model in brown color (Stolzenburg et al., 2025) and with the new multilayer model KM3C in blue color (Sect. S4). KM3C captures the observations assuming low diffusivity (10^{-20} cm^2 s^{-1}) in summer **(a)** and high diffusivity (10^{-15} cm^2 s^{-1}) in spring **(b)**. With the high and intermediate diffusivities assumed by Stolzenburg et al. (2025), the two-film model matches the observations in spring but not in summer (>10^{-15} cm^2 s^{-1}, solid brown line; 10^{-18} cm^2 s^{-1}, dashed brown line). Inserting the same low diffusivity as in KM3C (10^{-20} cm^2 s^{-1}), the two-film model can also match the summertime observations data for particles larger than 4 nm (dotted line). Note that all diffusivities listed for KM3C represent values at 298 K that are adjusted for temperature with $E_{a,dif} = 40$ kJ mol^{-1} in the model, while diffusivities in the two-film model are kept at their nominal values. Radial concentration profiles of sulfuric acid (H_2SO_4) and organic compounds with different volatilities (ULVOC, ELVOC, LVOC, SVOC) calculated by KM3C show that the growing particles (7 nm) are well-mixed and contain larger proportions of more volatile compounds (LVOC/SVOC) in spring **(d)**. In summer **(c)**, however, the growing particles contain larger proportions of less volatile compounds (ULVOC/ELVOC) and exhibit differential concentration gradients, which reflect kinetic limitations of mass transport ~~that were not captured by the two-film model~~.

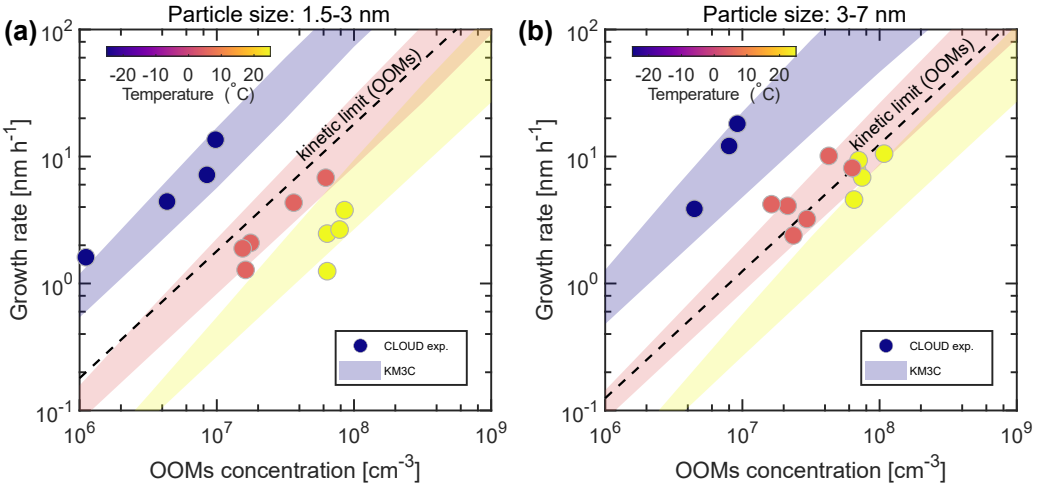

Figure 2. Secondary organic aerosol nanoparticle growth observed in laboratory experiments. Circular markers represent growth rates measured at different temperatures in the CERN CLOUD chamber (Stolzenburg et al., 2018, 2025) for particle size ranges of 1.5-3 nm **(a)** and 3-7 nm **(b)**. The dependence on temperature and concentration of oxygenated organic molecules (OOMs) determined by nitrate chemical ionization mass spectrometry (NO3-CIMS) was not captured by the modeling approach of Stolzenburg et al. (2025) (dashed line, "kinetic limit (OOMs)"). Considering also more volatile organic compounds detected by proton-transfer reaction time-of-flight mass spectrometry (PTR3, Stolzenburg et al. (2018)), volatility shifts according to the Clausius-Clapeyron equation, as well as variable particle-phase diffusivity, KM3C can reproduce both the temperature and concentration dependence (colored bands). The width of the colored bands corresponds to the same range of diffusivities as assumed in Fig. 1 (10^{-20} – 10^{-15} cm^2 s^{-1}, Sect. S5).

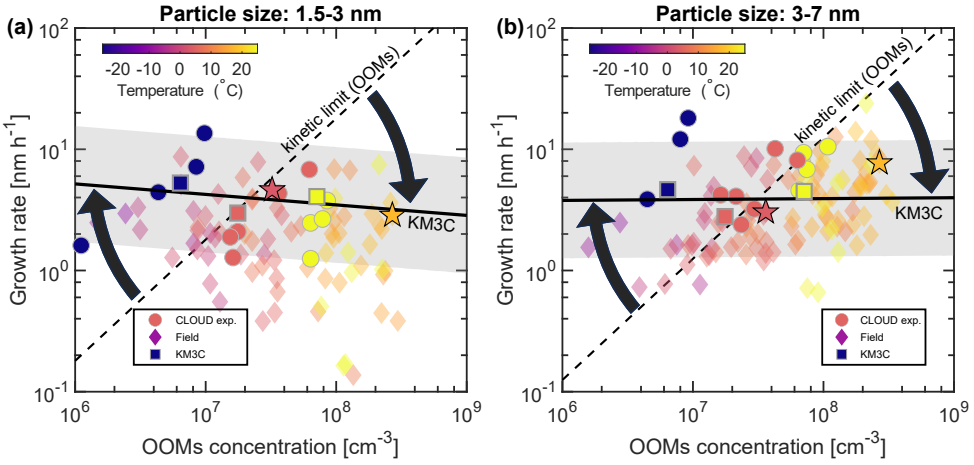

Figure 3. Range and buffering of observed and predicted atmospheric nanoparticle growth rates. Measurement data points color-coded by temperature represent growth rates as presented and discussed by Stolzenburg et al. (2025) for particles with diameters in the ranges of **(a)** 1.5-3 nm and **(b)** 3-7 nm, respectively. The data are plotted against the concentration of oxygenated organic molecules (OOMs) measured by NO3-CIMS during laboratory experiments in the CERN CLOUD chamber (circles, Stolzenburg et al., 2018) and during field measurements (diamonds) in Hyytiälä, Finland (Gonzalez Carracedo et al., 2022), Beijing, China (Qiao et al., 2021), and San Pietro di Capofiume, Italy (Cai et al., 2024). The two cases studied in Fig. 1 are highlighted with star-shaped markers. Square markers represent growth rates predicted by KM3C at the temperatures, median organic vapor concentrations and volatility distributions reported for the CERN CLOUD chamber experiments, and the solid black lines are linear fits to the model results. As indicated by the grey shaded areas, most of the growth rates observed in the field measurements and laboratory experiments fall within a factor of three relative to this line. The dashed black line is the kinetic limit reported by Stolzenburg et al. (2025), and the black arrows indicate the effective buffering of the organic vapor (OOMs) concentration dependence by temperature-related shifts in volatility and diffusivity.

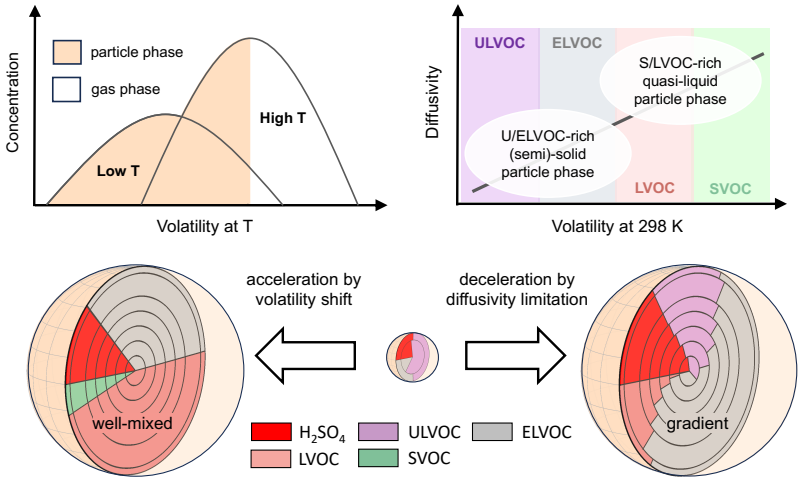

Figure 4. Key factors in the buffering of atmospheric nanoparticle growth rates. Ambient temperature influences the production and volatility distribution of condensable vapors in the atmosphere. An increase in temperature tends to enhance the production and concentration of organic vapors, but it also enhances their volatility (equilibrium vapor pressure) following the Clausius-Clapeyron equation and shifts the gas-particle partitioning towards the gas phase. These competing effects buffer the amount of vapors that are available to condense and drive particle growth. In addition, particle composition and phase state are influencing the molecular diffusivity, which tends to increase with increasing intrinsic volatility of the condensed organic compounds. At elevated temperatures, primarily very low volatile compounds (ULVOC, ELVOC) tend to condense and form (semi-)solid phases with kinetic limitations of diffusivity and surface-to-bulk transport, leading to differential concentration gradients and surface enrichment of more volatile compounds. At low temperatures, also more volatile compounds (SVOC, LVOC) tend to condense and favor the formation of quasi-liquid phases and well-mixed particles that are not subject to kinetic limitations by slow diffusion.